Check for updates

Transition of pulsed operation from Q-switching to continuous-wave mode-locking in a Yb:KLuW waveguide laser

JI EUN BAE,[1] XAVIER MATEOS,[2] MAGDALENA AGUILÓ,[2] FRANCESC DÍAZ,[2] JAVIER RODRÍGUEZ VÁZQUEZ DE ALDANA,[3] CAROLINA ROMERO,[3] HANSUEK LEE,[1,4] AND FABIAN ROTERMUND[1,*]

[1]*Department of Physics, Korea Advanced Institute of Science and Technology (KAIST), 34141 Daejeon, South Korea*
[2]*Física i Cristal·lografia de Materials i Nanomaterials (FiCMA-FiCNA), Universitat Rovira i Virgili (URV), 43007 Tarragona, Spain*
[3]*Aplicaciones del Láser y Fotónica, University of Salamanca, 37008 Salamanca, Spain*
[4]*Graduate School of Nanoscience and Technology, Korea Advanced Institute of Science and Technology (KAIST), 34141 Daejeon, South Korea*
[*]*rotermund@kaist.ac.kr*

Abstract: We report on the diverse pulsed operation regimes of a femtosecond-laser-written Yb:KLuW channel waveguide laser emitting near 1040 nm. By the precise position tuning of a carbon-nanotube-coated saturable absorber (SA) mirror, the transition of the pulsed operation from Q-switching, Q-switched mode-locking and finally sub-GHz continuous-wave mode-locking are obtained based on the interplay of dispersion and mode area control. The Q-switched pulses exhibit typical fast SA Q-switched pulse characteristics depending on absorbed pump powers. In the Q-switched mode-locking, amplitude modulations of the mode-locked pulses on the Q-switched envelope are observed. The radio-frequency spectrum represents the coexistence of Q-switching and mode-locking signals. In the purely mode-locked operation, the waveguide laser generates 2.05-ps pulses at 0.5 GHz.

1. Introduction

Waveguide (WG) structure is one of the most promising candidates for realizing miniaturized lasers. Compact high-repetition-rate mode-locked lasers have been actively investigated for their specific range of applications including integrated photonic circuits, frequency comb, astronomy and precise material processing [1–5]. In the 1-µm spectral region, ytterbium ions (Yb^{3+}) are attractive active dopants for diode-pumped high-power ultrafast lasers. In particular, monoclinic Yb^{3+}-doped potassium double tungstates such as $KLu(WO_4)_2$ (KLuW), $KY(WO_4)_2$ (KYW) and $KGd(WO_4)_2$ (KGW) possess the additional advantages of relatively broad and high absorption/emission cross-sections and exceptionally small Stokes shift (quantum defect) that lead to low thermal load and high laser efficiency. These benefits have attracted a lot of interest in them as suitable gain media for WG lasers [6–10]. The fabrication of channel WGs can be achieved via femtosecond direct laser writing (fs-DLW), which has been recognized as a promising technique that allows for strong confinement of the fundamental laser mode [7,10]. Recently, low-dimensional materials including nanocarbons, topological insulators and transition metal dichalcogenides have been successfully employed as saturable absorbers (SAs) in WG lasers for ultrashort pulse generation based on passively Q-switched mode-locking (QML) [11–17] or continuous-wave mode-locking (cw ML) [18–22]. Although semiconductor saturable absorber mirrors (SESAMs) are widely applied SAs, nanocarbons such as single-walled carbon

nanotubes (SWCNTs) and graphene provide unique optical properties, which can be integrated relatively easily into various laser systems. They benefit from their inherent broadband nonlinear absorption, ultrafast responses and flexibility for integration.

The practical utilization of pulsed lasers may require an adjustable pulsed regime (between Q-switching and mode-locking) that is amenable to control as well. It is well-known that a SA incorporated into a laser cavity can cause pure passive Q-switching, QML and cw ML. QML operation, which is usually accomplished by superimposing cw ML pulses on a Q-switched envelope, can produce bursts of ultrafast pulses at the Q-switched frequency (usually from kHz to MHz). Fully integrated investigations of such operation regime switching, including the modulation of mode-locked pulses in QML, have been recently demonstrated in certain types of laser [23–25]. However, systematic investigation on this aspect of WG lasers is still absent, although their specific advantages make them very suitable for practical applications mentioned earlier.

In this work, we report on the pulsed regime transition between passive Q-switching, QML and sub-GHz cw ML in a Yb:KLuW channel WG laser based on the combination of dispersion compensation and finely controlled mode area on SWCNT-SA. The results also show the first mode-locking results obtained using the Yb^{3+}-doped double tungstates WG laser, where a relatively simple extended cavity is used. The laser cavity consists of a focusing lens, fs-laser-written Yb:KLuW WG, output coupler and SWCNT-coated highly-reflecting (HR) mirror. The pulsed operation can be switched to different regimes by dispersion control through the Gires-Tournois interferometer (GTI) effect and the tuning of the laser mode area on the SWCNT-SA by using a piezo-actuator-controlled SWCNT-coated mirror. The characteristics of the Q-switched pulses are studied by varying the pump power and the amplitude modulation of the mode-locked pulses can be observed in the QML regime. The cw ML operation is finally achieved at a repetition rate of 0.50 GHz with pulse duration of 2.05 ps.

2. Experimental preparations and setup

The bulk 5 at.% Yb^{3+}-doped KLuW crystal was grown by the Top-Seeded-Solution Growth (TSSG) Slow-Cooling method using $K_2W_2O_7$ as a solvent [26]. The monoclinic Yb:KLuW (space group C^6_{2h} - C2/c) is optically biaxial. The crystal was oriented along the N_g axis (length of 2.53 mm) of the optical indicatrix to provide access to the high-gain $E \parallel N_m$ polarization (aperture 3.02 (N_m) × 2.93 (N_p) mm^2) being both uncoated $N_m \times N_p$ faces polished to laser-grade quality. The depressed-index channel WGs were fabricated in the bulk Yb:KLuW crystal by means of fs-DLW. To this aim, a Ti:sapphire regenerative amplifier emitting 120-fs pulses at 795 nm at a repetition rate of 1 kHz was employed. The laser beam was focused on the crystal using a 40× microscope objective (N.A. = 0.65) with an incident pulse energy adjusted to 74 nJ after the focusing optics. The sample scanning speed for inscription was 500 µm/s along its N_g axis producing damage tracks. The semicircular WG consisted of an undamaged core surrounded by a half-ring of damage tracks with a width of 18 µm near the crystal surface. We estimated the real part of the laser-induced refractive index change and the numerical aperture of the WG to be $\Delta n = n_{cladding} - n_{core} \approx -6 \times 10^{-4}$ and N.A. = 0.049, respectively. Figure 1(a) shows the optical microscope image of the WG. The lateral separation between inscribed adjacent tracks was 2 µm. The propagation loss in the WG was estimated by a modified Caird analysis [27] for a plane-parallel cavity with output coupling ratios of 1% to 20%. The resulting propagation loss amounts to ~0.56 dB/cm.

Arc-discharged SWCNTs (Meijo Nano Carbon Co., Ltd), which exhibit broadband nonlinear absorption in the 1-µm spectral range corresponding to the E_{22} interband transitions of SWCNTs were used as SAs. The SWCNT powders were dissolved in 1,2-dichlorobenzene (o-DCB) with a surfactant and agitated in an ultrasonicator. The solution was centrifuged for several minutes to remove the large bundles of nanotubes and impurities. The well-dispersed SWCNT solution was
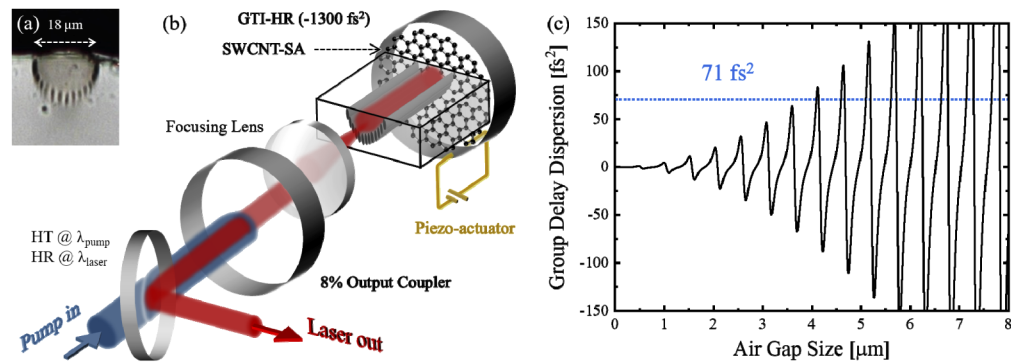
Fig. 1. (a) Optical microscope image of the Yb:KLuW WG with a channel width of 18 μm, (b) schematic of the Yb:KLuW channel WG laser and (c) calculated GTI effect in the WG laser.

then mixed with a separately prepared polymethyl methacrylate (Polymer Source, Inc.) solution (100 mg/ml in o-DCB) at a volume ratio of 1:1. The SWCNT composite was finally uniformly deposited on the HR mirror by spin-coating. The SWCNT-SA provides a modulation depth of ~1.3%, nonsaturable losses of ~3% and a saturation fluence of ~100 μJ/cm^2, while delivering a fast and slow decay time of about 200 fs and 2 ps, respectively.

The WG laser setup used in the experiment for all pulsed regimes is depicted in Fig. 1(b). The pump source is a tapered amplifier diode laser system (TA pro, Toptica Photonics, Inc.) centered at 981.6 nm. The pump beam passes through a half-wave plate, polarizer and another half-wave plate to linearly polarize it ($E \parallel N_m$) and attenuate the incident pump power. The collimated pump beam first passes through the output coupler (T = 8%) which is highly transparent at the pump wavelength. The beam is focused onto the front facet of the Yb:KLuW channel WG using a f = 20 mm plano-convex lens. The WG is mounted on a multi-axis stage without additional cooling. The end facet of the WG is closely attached parallel to the SWCNT-coated HR end mirror. This multifunctional HR mirror, whose GTI coating has a total group delay dispersion (GDD) of -1300 fs^2, is mounted on a piezoelectric actuator (PAZ005, Thorlabs) to control dispersion in the cavity by utilizing the GTI effect in the air-gap between the WG and the mirror. Theoretical calculations of the GTI effect in our laser setup lead to a period of ~522 nm as shown in Fig. 1(c). In addition, the laser mode area on the SWCNT-SA is also controlled to switch the pulsed regime by considering the criterion for switching between QML and cw ML [28]. The optical cavity length of the laser in the present cavity configuration is 30 cm, which leads to the experimentally achieved fundamental mode-locked frequency of 0.5 GHz.

3. Experimental results and discussion

Figure 2 shows the transition of different pulsed operation regimes of the Yb:KLuW channel WG laser at the maximum power, from pure Q-switching and QML to finally cw ML. In the first regime (Fig. 2(a)), the purely Q-switched pulses obtained during stable operation display typical fast-SA Q-switched pulse characteristics, depending on the absorbed pump power as shown in Fig. 3. The Q-switched pulse repetition rate and pulse duration (at full-width at half-maximum (FWHM)) are measured directly from the oscilloscope trace (1-GHz Tektronix, TDS784D) using a fast InGaAs photodiode. The pulse duration decreases from 2400 to 860 ns as the pump power increases, while the repetition rate increases from 87 to 235 kHz. A maximum peak power of 3.70 W and a corresponding pulse energy of 3.18 μJ are obtained. The operating wavelength of the Q-switched pulse is ~1046 nm.
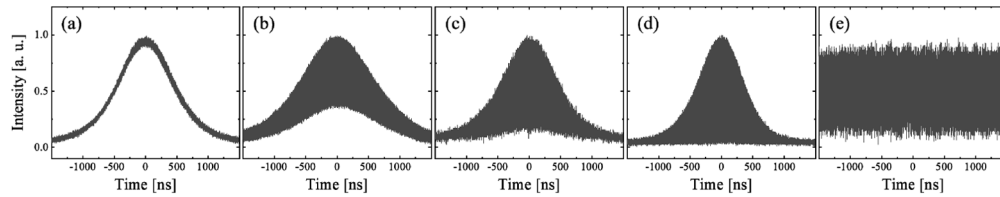
Fig. 2. Transition of pulsed operation switching of the Yb:KLuW WG laser at the maximum pump power: (a) pure Q-switching, (b-d) QML including the amplitude modulation of mode-locked pulses and (e) cw ML.
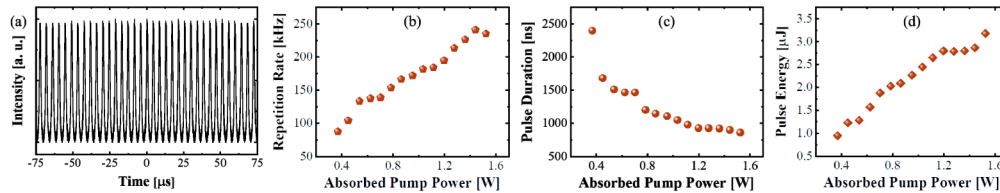
Fig. 3. (a) Q-switched pulse train at the maximum pump power and (b-d) Q-switched laser characteristics as a function of the absorbed pump power.

The QML operation generates amplitude-modulated ultrafast pulses on the Q-switched pulse envelope, as shown in Figs. 2(b)–2(d). In particular, a close look at the fully-modulated case (Fig. 2(d)) shows mode-locked pulses with a repetition rate of ∼0.50 GHz which corresponds to the effective cavity length of the WG laser as shown in Fig. 4(a). This can also be confirmed by the radio-frequency (RF) spectrum measured by a signal and spectrum analyzer (FSW26, Rohde & Schwarz Inc.) with a resolution bandwidth (RBW) of 1 kHz. These measurements show the coexistence of the mode-locked frequency and the harmonics of Q-switched frequency, as shown in Fig. 4(b). The Q-switched repetition rate at 0.23 MHz exhibits the strongest peak with clear high harmonics. The fundamental beat note in the mode-locked repetition rate centered at 0.496 GHz shows a strong RF peak with an extinction ratio of 57 dB, with the side frequency components of the Q-switched envelope.
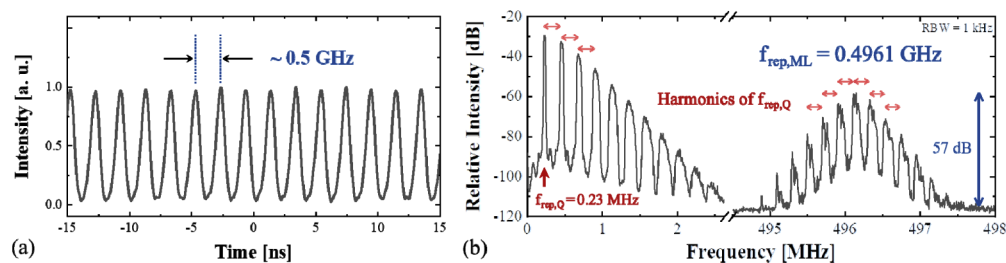

Fig. 4. (a) Mode-locked pulses on the Q-switched pulse envelope, indicating fully-modulated QML pulses and (b) RF spectrum of the QML pulses, showing the harmonics of the Q-switched frequency and the mode-locked frequency.

In the case of the cw ML regime, the Q-switched operation is fully suppressed as shown in the pulse train of Fig. 2(e). Figure 5(a) displays the recorded mode-locked pulse train at a repetition rate of ∼0.50 GHz showing the pulse-to-pulse stability of ∼12%. In Fig. 5(b), the fundamental RF peak at ∼0.50 GHz, measured with a RBW of 1 kHz, shows an extinction ratio of 56 dB without any Q-switching signals or instabilities, indicating stable purely cw ML operation. The

measured autocorrelation trace of the pulses, shown in Fig. 5(c), leads to a pulse duration of 2.05 ps assuming Gaussian pulse shapes. The corresponding spectrum with a FWHM spectral bandwidth of 0.84 nm is centered at 1042.3 nm (Fig. 6(a)). The resulting time-bandwidth product is 0.473, close to the theoretical Fourier limit of 0.441. The accumulated GDD in the cw ML operation is about -473 fs^2 while the total cavity GDD is estimated to be about -544 fs^2 when the dispersion of Yb:KLuW crystal (+110 fs^2/mm), focusing lens (+24.3 fs^2/mm), air (+0.017 fs^2/mm) and GTI-HR mirror (-1300 fs^2 per bounce) was taken into account without GTI effect in the air gap between the WG and SWCNT-coated GTI-HR mirror. This result leads us to infer that the GDD induced by the GTI effect is about 71 fs^2 (Fig. 1(c)).
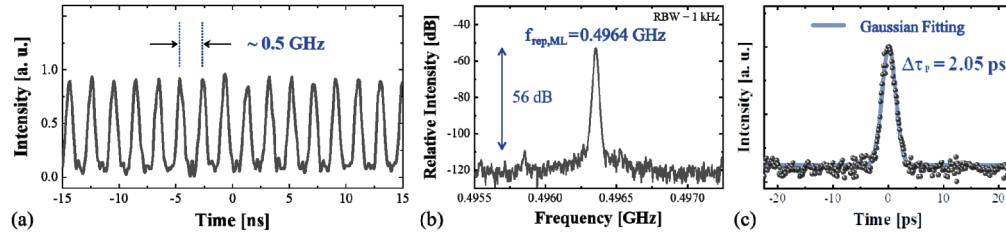
Fig. 5. (a) Measured cw ML pulse train, (b) RF spectrum of the cw ML pulses and (c) autocorrelation trace with Gaussian fit.
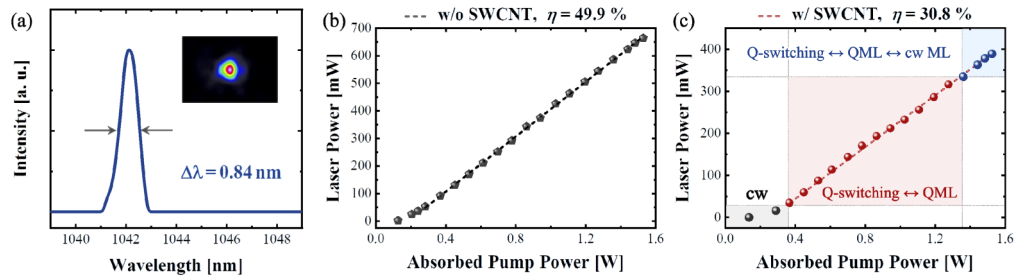
Fig. 6. (a) Spectrum of the cw ML pulse (inset: beam profile at the maximum power). Average output power characteristics as a function of the absorbed pump power in the (b) cw and (c) pulsed regime.

The piezo-controlled SWCNT-coated HR mirror plays a key role for switching to different pulsed regimes. First, the GDD can be properly adjusted to obtain sufficient modulation for mode-locking using the GTI effect. In addition, the mode area in the SWCNT-SA can be controlled by the position-dependent laser beam divergence in the air gap between the WG and the SWCNT-coated end mirror to meet the stability criterion for the QML and cw ML operation [28]. The criterion for critical intracavity pulse energy E_p can be expressed as $E_p = (E_{sat,L}\cdot E_{sat,A}\cdot\Delta R)^{1/2}$, where $E_{sat,L/A}$ is the saturation energy of gain medium/SA and ΔR is the modulation depth of SA, while $E_{sat,A}$ is the product of the saturation fluence and mode area at the SA. It should be noted that the mode area can be changed by piezo-controlling the position of the end mirror. Assuming that the other laser parameters are fixed and the variation in the air gap ranges from 50 to 200 μm, the mode radius variation on the SWCNT-SA is to be between 8.24 and 11.1 μm. The resulting critical E_p value then lies between 7.92 and 10.7 nJ. At the maximum pump power, the experimental E_p is ~9.80 nJ. Consequently, we were able to switch the pulsed operation regime between QML and cw ML via precise adjustments of the air gap to approach the intracavity pulse energy.

Figures 6(b) and 6(c) show the input-output power dependence in the cw operation without SWCNT-SA and pulsed operation employing SWCNT-SA. The absorbed pump power is estimated by considering the Fresnel losses at the WG facets and the absorption under the lasing condition. The cw ML threshold is measured at the absorbed pump power of 1.35 W. The laser power at the threshold value leads to E_p of 8.43 nJ, which matches well with the range of the critical E_p calculated above. Thus, in the region of higher powers (the blue region in Fig. 6(c)), we can achieve all pulsed operation regimes by adjusting the position of the SWCNT-coated end mirror. In the region of lower powers, switching between Q-switched and QML operation can be achieved. The cw and pulsed operations deliver maximum laser powers of 663 and 389 mW with slope efficiency η of 49.9% and 30.8%, respectively. The results indicate very high output powers and slope efficiency for cw ML WG lasers. Note that the polarization states of the output beam both in cw and pulsed operations are same as that of the pump polarization $E \parallel N_m$. The measured laser spectrum of the cw ML pulses is shown in Fig. 6(a). The spectrum can be slightly shifted depending on the air-gap size in a period of about 540 nm, which corresponds to the periodicity of the GTI effect. The cw ML laser beam profile measured at the maximum pump power is a fundamental mode as shown in the inset of Fig. 6(a).

4. Conclusion

We demonstrate Q-switched, QML and sub-GHz cw ML operation in a fs-laser-written Yb:KLuW channel WG laser by employing SWCNT-SA and simultaneously investigate the transition between different operation regimes. We achieved a cw ML Yb^{3+}-doped double tungstates WG laser for the first time using a relatively simple extended cavity configuration. The precisely adjusted position of the piezo-controlled SWCNT-coated end mirror enables the switching of the pulsed operation regime by controlling the dispersion through the GTI effect and the laser mode area on SA. In terms of SA choice, SWCNT is a very suitable material to study transition characteristics of the pulsed regime thanks to precisely controllable SA parameters compared to other nanomaterials. The mode-locked laser delivers high average output powers up to 389 mW at 1042.3 nm with a slope efficiency of 30.8%. The WG laser generates 2.05-ps pulses at a repetition rate of 0.50 GHz. The transition characteristics of the operation regime in a compact WG laser format reported in this study can be beneficial for diverse practical applications. Since the dispersion and the mode area are very sensitive to the air gap size, further optimization of SA parameters and precise dispersion management can produce much shorter pulses. In addition, based on merits of the surface channel WG structure, evanescent-field interaction with the SA deposited on top of the WG will be the next step to demonstrate stable high-power mode-locked operation.

Funding

Disclosures

The authors declare no conflicts of interest.

References

1. T. M. Fortier, A. Bartels, and S. A. Diddams, "Octave-spanning Ti:sapphire laser with a repetition rate >1 GHz for optical frequency measurements and comparisons," Opt. Lett. **31**(7), 1011–1013 (2006).
2. R. Aviles-Espinosa, G. Filippidis, C. Hamilton, G. Malcolm, K. J. Weingarten, T. Sudmeyer, Y. Barbarin, U. Keller, S. I. Santos, D. Artigas, and P. Loza-Alvarez, "Compact ultrafast semiconductor disk laser: targeting GFP based nonlinear applications in living organisms," Biomed. Opt. Express **2**(4), 739–747 (2011).

3. M. P. Moreno and S. S. Vianna, "Femtosecond 1 GHz Ti:sapphire laser as a tool for coherent spectroscopy in atomic vapor," J. Opt. Soc. Am. B **28**(9), 2066–2069 (2011).

4. C. Kerse, H. Kalaycioglu, P. Elahi, B. Cetin, D. K. Kesim, O. Akcaalan, S. Yavas, M. D. Asik, B. Oktem, H. Hoogland, R. Holzwarth, and F. O. Ilday, "Ablation-cooled material removal with ultrafast bursts of pulses," Nature **537**(7618), 84–88 (2016).

5. R. A. McCracken, J. M. Charsley, and D. T. Reid, "A decade of astrocombs: recent advances in frequency combs for astronomy," Opt. Express **25**(13), 15058–15078 (2017).

6. M. Pollnau, Y. E. Romanyuk, F. Gardillou, C. N. Borca, U. Griebner, S. Rivier, and V. Petrov, "Double tungstate lasers: From bulk toward on-chip integrated waveguide devices," IEEE J. Sel. Top. Quantum Electron. **13**(3), 661–671 (2007).

7. F. M. Bain, A. A. Lagatsky, R. R. Thomson, N. D. Psaila, N. V. Kuleshov, A. K. Kar, W. Sibbett, and C. T. A. Brown, "Ultrafast laser inscribed Yb:KGd(WO$_4$)$_2$ and Yb:KY(WO$_4$)$_2$ channel waveguide lasers," Opt. Express **17**(25), 22417–22422 (2009).

8. J. M. de Mendívil, J. del Hoyo, J. Solís, M. C. Pujol, M. Aguiló, F. Díaz, and G. Lifante, "Mirrorless Yb^{3+}-doped monoclinic double tungstate waveguide laser combining liquid phase epitaxy and multiplexed beam fs laser writing," J. Lightwave Technol. **33**(23), 4726–4730 (2015).

9. J. W. Kim, S. Y. Choi, J. E. Bae, M. H. Kim, Y. U. Jeong, E. Kifle, X. Mateos, M. Aguiló, F. Díaz, U. Griebner, V. Petrov, G. H. Kim, and F. Rotermund, "Comparative study of Yb:KYW planar waveguide lasers Q-switched by direct- and evanescent-field interaction with carbon nanotubes," Opt. Express **27**(2), 1488–1496 (2019).

10. J. E. Bae, T. G. Park, E. Kifle, X. Mateos, M. Aguiló, F. Díaz, C. Romero, J. R. V. de Aldana, H. Lee, and F. Rotermund, "Carbon nanotube Q-switched Yb:KLuW surface channel waveguide lasers," Opt. Lett. **45**(1), 216–219 (2020).

11. R. Mary, G. Brown, S. J. Beecher, F. Torrisi, S. Milana, D. Popa, T. Hasan, Z. Sun, E. Lidorikis, S. Ohara, A. C. Ferrari, and A. K. Kar, "1.5 GHz picosecond pulse generation from a monolithic waveguide laser with a graphene-film saturable output coupler," Opt. Express **21**(7), 7943–7950 (2013).

12. Y. Ren, G. Brown, R. Mary, G. Demetriou, D. Popa, F. Torrisi, A. C. Ferrari, F. Chen, and A. K. Kar, "7.8-GHz graphene-based 2-μm monolithic waveguide laser," IEEE J. Sel. Top. Quantum Electron. **21**(1), 395–400 (2015).

13. A. Choudhary, S. Dhingra, B. D'Urso, P. Kannan, and D. P. Shepherd, "Graphene Q-Switched Mode-Locked and Q-Switched Ion-Exchanged Waveguide Lasers," IEEE Photon. Technol. Lett. **27**(6), 646–649 (2015).

14. X. Jiang, S. Gross, H. Zhang, Z. Guo, M. J. Withford, and A. Fuerbach, "Bismuth telluride topological insulator nanosheet saturable absorbers for q-switched mode-locked Tm:ZBLAN waveguide lasers,"," Ann. Phys. **528**(7-8), 543–550 (2016).

15. F. Thorburn, A. Lancaster, S. McDaniel, G. Cook, and A. K. Kar, "5.9 GHz graphene based q-switched modelocked mid-infrared monolithic waveguide laser," Opt. Express **25**(21), 26166–26174 (2017).

16. X. T. Jiang, S. Gross, M. J. Withford, H. Zhang, D. I. Yeom, F. Rotermund, and A. Fuerbach, "Low-dimensional nanomaterial saturable absorbers for ultrashort-pulsed waveguide lasers," Opt. Mater. Express **8**(10), 3055–3071 (2018).

17. Z. Q. Li, Y. X. Zhang, C. Cheng, H. H. Yu, and F. Chen, "6.5 GHz Q-switched mode-locked waveguide lasers based on two-dimensional materials as saturable absorbers," Opt. Express **26**(9), 11321–11330 (2018).

18. A. G. Okhrimchuk and P. A. Obraztsov, "11-GHz waveguide Nd:YAG laser CW mode-locked with single-layer graphene," Sci. Rep. **5**(1), 11172 (2015).

19. S. Y. Choi, T. Calmano, F. Rotermund, and C. Kränkel, "2-GHz carbon nanotube mode-locked Yb:YAG channel waveguide laser," Opt. Express **26**(5), 5140–5145 (2018).

20. C. Grivas, R. Ismaeel, C. Corbari, C. C. Huang, D. W. Hewak, P. Lagoudakis, and G. Brambilla, "Generation of Multi-Gigahertz Trains of Phase-Coherent Femtosecond Laser Pulses in Ti:Sapphire Waveguides," Laser Photonics Rev. **12**(11), 1800167 (2018).

21. Z. Li, N. Dong, Y. Zhang, J. Wang, H. Yu, and F. Chen, "Mode-locked waveguide lasers modulated by rhenium diselenide as a new saturable absorber," APL Photonics **3**(8), 080802 (2018).

22. M. V. Ponarina, A. G. Okhrimchuk, M. G. Rybin, M. P. Smayev, E. D. Obraztsova, A. V. Smirnov, I. V. Zhluktova, V. A. Kamynin, T. V. Dolmatov, V. V. Bukin, and P. A. Obraztsov, "Dual-wavelength generation of picosecond pulses with 9.8 GHz repetition rate in Nd:YAG waveguide laser with graphene,"," Quantum Electron. **49**(4), 365–370 (2019).

23. J. Lee, J. Koo, Y. M. Chang, P. Debnath, Y. W. Song, and J. H. Lee, "Experimental investigation on a Q-switched, mode-locked fiber laser based on the combination of active mode locking and passive Q switching," J. Opt. Soc. Am. B **29**(6), 1479–1485 (2012).

24. M. J. Strain, M. Zanola, G. Mezosi, and M. Sorel, "Ultrashort Q-switched pulses from a passively mode-locked distributed Bragg reflector semiconductor laser," Opt. Lett. **37**(22), 4732–4734 (2012).

25. X. Li, H. Wang, Z. Qiao, X. Guo, W. Wang, G. I. Ng, Y. Zhang, Y. Xu, Z. Niu, C. Tong, and C. Liu, "Investigation of regime switching from mode locking to Q-switching in a 2 μm InGaSb/AlGaAsSb quantum well laser," Opt. Express **26**(7), 8289–8295 (2018).

26. V. Petrov, M. C. Pujol, X. Mateos, Ò Silvestre, S. Rivier, M. Aguiló, R. M. Solé, J. H. Liu, U. Griebner, and F. Díaz, "Growth and properties of KLu(WO$_4$)$_2$, and novel ytterbium and thulium lasers based on this monoclinic crystalline host," Laser Photonics Rev. **1**(2), 179–212 (2007).

27. J. A. Caird, S. A. Payne, P. R. Staver, A. J. Ramponi, L. L. Chase, and W. F. Krupke, "Quantum electronic properties of the $Na_3Ga_2Li_3F_{12}$:Cr^{3+} Laser," IEEE J. Quantum Electron. **24**(6), 1077–1099 (1988).

28. C. Hönninger, R. Paschotta, F. Morier-Genoud, M. Moser, and U. Keller, "Q-switching stability limits of continuous-wave passive mode locking," J. Opt. Soc. Am. B **16**(1), 46–56 (1999).